Carbohydrate Polymers 92 (2013) 128–137

Contents lists available at SciVerse ScienceDirect

Carbohydrate Polymers

journal homepage: www.elsevier.com/locate/carbpol

# The relation of apple texture with cell wall nanostructure studied using an atomic force microscope

Justyna Cybulska [a,*], Artur Zdunek [a], Katarzyna M. Psonka-Antonczyk [b], Bjørn T. Stokke [b]

[a] Institute of Agrophysics, Polish Academy of Sciences, Doswiadczalna 4, 20-290 Lublin, Poland
[b] Biophysics and Medical Technology, Department of Physics, Norwegian University of Science and Technology, NO-7491 Trondheim, Norway

ARTICLE INFO

*Article history:*
Received 3 April 2012
Received in revised form 21 August 2012
Accepted 26 August 2012
Available online 7 September 2012

*Keywords:*
Cell wall
Cellulose
Texture
Firmness
Apple
Atomic force microscopy

ABSTRACT

In this study, the relation of the nanostructure of cell walls with their texture was investigated for six different apple cultivars. Cell wall material (CWM) and cellulose microfibrils were imaged by atomic force microscope (AFM). The mean diameter of cellulose microfibrils for each cultivar was estimated based on the AFM height topographs obtained using the tapping mode of dried specimens. Additionally, crystallinity of cellulose microfibrils and pectin content was determined. Texture of apple cultivars was evaluated by sensory and instrumental analysis. Differences in cellulose diameter as determined from the AFM height topographs of the nanostructure of cell walls of the apple cultivars are found to relate to the degree of crystallinity and pectin content. Cultivars with thicker cellulose microfibrils also revealed crisper, harder and juicier texture, and greater acoustic emission. The data suggest that microfibril thickness affects the mechanical strength of cell walls which has consequences for sensory and instrumental texture.



## 1. Introduction

Many macroscopic properties and sensory qualities of plant foods relate to the micro- and nanostructure (Aguilera, 2005; Brummell & Harpster, 2001). Cell walls, beside turgor pressure, are the main architecture responsible for the texture of fruit and vegetable parenchyma tissue. The texture, in particular sensory attributes such as crispness, hardness and juiciness, determine consumer acceptance and usefulness in numerous technological processes. Moreover, cell walls are a valuable component of one's daily diet as dietary fibre since they contribute to the correct functioning of the alimentary canal and thereby reduce the tendency toward obesity (Jarvis, 2011).

The cell walls of apple parenchyma have an advantageous chemical composition from the dietary and mechanical point of view. Apple cell walls are composed mostly of polysaccharides; they can include 40% pectin, 25% hemicelluloses (the dominant hemicellulose in apple parenchyma is xyloglucan) and 20% cellulose (Brummell & Harpster, 2001):

1. Cellulose is composed of (1-4)-β-linked D-glucose chains, assembled together by hydrogen bonding into long crystalline microfibrils. Cellulose microfibrils involve a highly crystalline core surrounded by less crystalline regions and interrupted by amorphous forms of cellulose.
2. Hemicellulose occurs in cell walls in various forms, such as xyloglucan, glucomannan and glucuronoarabinoxylan, with xyloglucan being the most abundant. Xyloglucan coats cellulose microfibrils by hydrogen bonding and spans adjacent microfibrils, thereby linking them together. Because xyloglucan forms long chains (hundreds of micrometres), this polymer plays a significant role in cell wall mechanics. Others hemicelluloses, less abundant in the primary cell walls of dicotyledonous plants, also cross-link microfibrils by hydrogen bonding, although more weakly than xyloglucan.
3. Pectins are a complex polysaccharide rich in galacturonic acid which occur in the primary cell walls in the three distinct forms of homogalacturonan, rhamnogalacturonan I and rhamnogalacturonan II. The most abundant pectin in apple and pear parenchyma is homogalacturonan, which usually is initially highly methyl-esterified. Pectins, normally largely hydrated, fill the space between the cellulose/xyloglucan network. They also form a network, linked together by ester bonds between pectin molecules and by ionic calcium bridges between de-methyl-esterified homogalacturonans (Cybulska, Zdunek, & Konstankiewicz, 2011).

The macromolecules are organized in a complex network supporting numerous functionalities and with architecture that have a significant influence on the whole parenchyma system, including

* Corresponding author. Tel.: +48 81 744 50 61; fax: +48 81 744 50 67.
*E-mail address:* j.cybulska@ipan.lublin.pl (J. Cybulska).

0144-8617/$ – see front matter © 2012 Elsevier Ltd. All rights reserved.
http://dx.doi.org/10.1016/j.carbpol.2012.08.103

mechanical properties. However, it must be emphasized that the exact role of each polysaccharide and the interactions between them are still under discussion. According to one of the recent cell wall models, pectins form an independent network, in parallel to that of the cross-linking glycans, which works as a plasticizer and water binding agent (Cybulska, Vanstreels, et al., 2010). The role of pectin and cross-linking glycans is to bind to cellulose microfibrils in the cell wall. In an alternate cell wall model, pectins also interact with cellulose, however, they compete with glycans (Żykwińska, Thibault, & Ralet, 2008). When xyloglucan concentration is high, pectin absorption onto cellulose is lower, thus the cellulose–pectin interactions are weaker than interactions between cellulose and xyloglucan, whereas at low xyloglucan abundance, the main function of pectins is to bind the gap between microfibrils.

Analysis of the cell wall structure requires microscopes that allow observation at the nanometre scale due to the dimensions of the polysaccharides macromolecules. The atomic force microscope (AFM) has been shown to be a very useful tool for observing the molecular structure of a single macromolecule and cell wall assemblies (Cybulska, Konstankiewicz, Zdunek, & Skrzypiec, 2010; Cybulska, Vanstreels, et al., 2010; Morris et al., 1997) with minimal sample preparation (Kirby, Gunning, Waldron, Morris, & Ng, 1996). AFM provides much valuable information which was not always obtainable by analytical methods (Round, Rigby, MacDougall, & Morris, 2010; Zhang et al., 2012). Davies and Harris (2003) applied AFM to measure cellulose microfibrils in partially hydrated sampled of model dicotyledon *Arabidopsis thaliana* and monocotyledon – onion. Water content in cells significantly influences the diameter of cellulose microfibril which was documented in the experiment with different water levels of hydrations (Thimm, Burritt, Ducker, & Melton, 2000). Changes of arrangement of the cellulose microfibrils of growing cucumber cells were investigated by means of AFM (Marga, Grandbois, Cosgrove, & Baskin, 2005). Based on AFM observation, a model of a 36-chain elementary cellulose fibril and its biosynthesis of the maize parenchyma cell wall was proposed (Ding & Himmel, 2006). AFM was also used for studying the action of cellulases enzyme on cellulose which showed an increase in the proportion of crystalline regions during hydrolysis (Liu, Fu, Zhu, Li, & Zhan, 2009). Differences in the nanostructure of commercial citrus pectin, orange albedo pectin and lime albedo pectin were described quantitatively with the use of AFM imaging (Fishman, Cooke, & Coffin, 2006). Degradation of water-soluble pectin was detected using AFM on the basis of pectin aggregates separation (Yang, An, Feng, Li, & Lai, 2005). Pectin–protein complexes, found in extractions from unripe tomato, can play the role of emulsifying factors (Kirby, MacDougall, & Morris, 2008). AFM allowed observation of changes of pectin chains after fruit storage and $Ca^{2+}$ treatment (Liu, Chen, et al., 2009). It shown that immersion of the strawberry fruit in a $Ca^{2+}$ solution delays undesired physicochemical changes, as well as degradation of pectins, by strengthening the ionic cross-linkages among pectin molecules (Chen et al., 2011). Hydrolysis of pectin was analysed on the basis of the backbone length, branching and branch length distributions for individual polymers (Round et al., 2010).

So far, AFM has been used mainly for comparison of nanostructures among different species. Very rarely are differences between cultivars within the same commodity analysed from the point of view of nanostructure of cell walls. Recently, Zhang et al. (2010) showed differences in nanostructure of pectins between soft and crispy peach cultivars which was also related to differing firmness of these cultivars, whereas Chen et al. (2009) found differences between the nanostructure of hemicelluose macromolecules of crisp and soft Chinese cherry cultivars. At present, a degradation of pectins in the cell wall and middle lamella is considered as the main factor determining the dynamics of fruits softening. However, the properties of cellulose microfibres, like diameter or degree of crystallinity, or their spatial assembly, have not been investigated with relation to the macromechanical properties of fruit tissue. This is particularly important in the case of apples due to the wide range of available cultivars which differ in terms of sensory texture. The crystallinity degree of cellulose has not been considered yet as an important factor influencing fruit texture, however, the presence of crystal and amorphous parts of microfibrils is important with regard to the interaction with other biopolymers and water binding capacity. Therefore, in this study, firstly six apple varieties at approximately the same stage of ripening were investigated to verify whether significant differences exist in terms of their cell wall nanostructure properties: cellulose microfibrils' diameter, cellulose crystallinity and pectin content. Then, the nanostructure properties were compared with sensory texture attributes and instrumental parameters often used for texture evaluation.

## 2. Materials and methods

### 2.1. Materials

Six apple [*Malus x domestica* (Borkh.)] cultivars were used in the experiment: 'Cortland', 'Honeycrisp', 'Ligol', 'Mutsu', 'Rubin' and 'Jonagold'. Fruits were purchased from the orchard of the Research Institute of Pomology and Floriculture in Skierniewice, Poland. The apples have been harvested at the optimum maturity time for each cultivar based on ethylene test from seeds ovary and starch iodine test (Konopacka & Płocharski, 2004). Before experiment the apples were stored at 2 °C in a normal atmosphere for two months after harvest.

### 2.2. Cell wall material (CWM) and cellulose isolation

Apple cell wall material (CWM) was isolated using the modified phenol buffer method proposed by Renard (2005). Frozen apple slices were homogenized in a cold buffer, simulating the ionic conditions in apple juice (1.2 mM $CaCl_2$, 2.0 mM $MgCl_2$, 0.5 g $L^{-1}$ KCl, 60 mg $L^{-1}$ ascorbic acid, 4 g $L^{-1}$ apple acid, 1 g $L^{-1}$ sodium disulphite supplemented to pH 3.5 with 5 M NaOH) with Triton 100 (2 g $L^{-1}$) and 1-octanol (4 mL). The suspension was then filtered under reduced pressure and washed in a 60% water solution of acetone. The resultant paste was blended with phenol at a volumetric ratio of 1:4 and left for 1 h at room temperature. Next, the blend was dissolved in the buffer and filtered. The material was washed successively in 70% and 96% ethanol, and finally in acetone.

Cellulose from apple tissue was obtained during sequential extraction of cell walls in order to remove pectin and hemicelluloses according to the method proposed by Redgwell, Melton, and Brasch (1988) with some modifications. Cell walls were stirred in deionized water for 6 h at 20 °C and then in 0.1 M cyclohexane-trans-1.2-diamine tetra-acetate (CDTA) (pH 6.5) at 25 °C for 2 h, since 6 h after the previous step. Then the residue was diluted in 0.05 M sodium carbonate ($Na_2CO_3$) with addition of 20 mM sodium borohydride ($NaBH_4$) and stirred for approx. 20 h at 1 °C, filtered, and again stirred for 2 h at 20 °C. After filtration, depectinated cell walls were stirred sequentially in 0.5 M, 1 M and 4 M of potassium hydroxide (KOH) with an addition of 20 mM $NaBH_4$ each for 2 h at 20 °C every time. Finally all cellulose from the apple tissue was rinsed several times in deionized water and ethanol.

### 2.3. Pectin content determination

Supernatants after CDTA and $Na_2CO_3$ treatment were used for pectin determination. Galacturonic acid content was

automatically determined with a San$^{++}$ Continuous Flow Analyzer (Skalar, The Netherlands) according to the colorimetric method by Blumenkrantz and Asboe-Hansen (1973). The sample was totally decomposed in 96% sulphuric acid ($H_2SO_4$) with di-sodium tetra borate $Na_2B_4O_7{\cdot}10H_2O$. Then the products were transformed to furfuric derivatives. The derivatives react with the 3-phenyl phenol to form a coloured dye, which is measured at 530 nm. Mono-galacturonic acid solutions (10–100 μg/mL) were used as a standard calibration curve.

### 2.4. AFM observations

CWM's and cellulose isolated from the pulp made of 10 apples of each cultivar were observed by means of the atomic force microscope (BioScope Catalyst, Veeco Instruments Inc.). Suspension of CWM or cellulose in 50% ethanol was poured onto microscope glasses. Five preparations have been made for each sample. Then preparations were vacuum dried at $1.3 \times 10^{-4}$ Pa for at least 4 h prior to being imaged by AFM. AFM topographs of size 2 μm × 2 μm were taken in air in the tapping mode with tapping mode silicon cantilevers RTESP (Veeco Instruments Inc.), with nominal spring constant between 20 and 80 N/m. The height topographs were flattened line by line using Nanoscope 8.0 software (Veeco Instruments Inc.). AFM images were analysed quantitatively by means of WSxM 4.0 Develop 8.0 software (Nanotec Electronica, Madrid, Spain). This software is designed for scanning probe microscopy, including atomic force microscopy (Horcas et al., 2007).

The diameter of microfibrils from cellulosic samples was determined on the basis of the two-dimensional height topographs as described by Cybulska, Vanstreels, et al. (2010). Linear sections were marked out randomly on the images and used as the basis for the automatic extraction of height profiles. The width of the peaks was measured on the obtained profiles. It was assumed that the each peak represents one cellulose microfibril. The mean diameter of microfibrils was determined from approximately 50 randomly chosen microfibrils from 5 images for each sample. The root mean square (RMS) roughness was determined automatically for each AFM image on the basis of histograms which performed the distribution of the height of structural elements from the 2D height topographs.

### 2.5. Degree of cellulose crystallinity

Degree of crystallinity was determined by means of the X-ray diffraction method. The X-ray diffractometer HZG - 4 (Carl Zeiss Jena, Germany) was used. Samples were scanned with Cu $K_\alpha$ radiation ($\lambda = 0.15418$ nm). The parameters of the working lamp were as follows: $U = 33$ kV, $I = 22$ mA. The intensity of reflections was measured over the angular 6–60° $2\theta$ with step intervals of 0.04°. The duration of the reflection count was 10 s. On the basis of registered measurements, a mathematic model describing the relationship between intensity and $2\theta$ was developed. The Pearson VII function was used for mathematic description of every single reflection. Calculated models of the diffractograms were applied to quantify the degree of cellulose crystallinity. The degree of crystallinity was calculated according to the general equation given by Wunderlich (1973):

$$\mathrm{Xc} = \frac{I_c}{I_c + kI_a} \times 100\%,$$

where Xc – degree of crystallinity, $I_c$ – area under the reflex from the crystalline phase, $I_a$ – spectrum area of the amorphous phase, $k$ – proportionality factor including polarization and Lorenz effect (Thompson–Lorenz factor), temperature correction and differences between X-ray density of amorphous phase.

### 2.6. Sensory analysis

Sensory analysis was performed using generic descriptive analysis in the laboratory working according to the general requirements of the relevant ISO 8589:1998 (1998) standard for sensory testing conditions. Each test booth is equipped with a computerized system for data acquisition (Analsens v.4 software, Caret Systemy Cyfrowe i Oprogramowanie SP z o.o., Gdansk, Poland).

The expert panel was recruited from staff at the Institute of Agrophysics and was selected on the basis of the ability of individuals to discriminate taste and texture attributes. Panellists have been trained by external expert on apples and pears of different texture and appearance to evaluate a large set of texture, taste and colour properties of fruits by using the generic descriptive method (Lawless & Heymann, 2010). The team participate in a few projects concerning apple texture. Additionally, before the experiment, the panellists took part in a refresher session, where definitions of fruit texture attributes were discussed and clarified again. Ten panellists took part in the sensory tests. Ten apples of each cultivar were used for sensory evaluation. The following texture attributes were determined by the panellists: crispness, hardness and juiciness according to definitions described by Zdunek, Cybulska, Konopacka, and Rutkowski (2010). During one sensory session, each person tested 1 sample (two quarters of an apple) from each batch (12 samples per session per panellists). Each piece of apple was assigned a 3-digit code and the samples were presented in random order. However panellist received two coded samples of each cultivar. The panellists determined the perceived intensity of texture attributes using a linear, unstructured scale with a range of 0–100 points. After the test, the results were converted to the most frequently used 10-point scale.

### 2.7. Instrumental evaluation with CAED

Before sensory analysis the same apples were used for instrumental evaluation with contact acoustic emission detector (CAED). CAED measures firmness and acoustic emission (Zdunek et al., 2010; Zdunek, Cybulska, Konopacka, & Rutkowski, 2011a, 2011b). The device uses a force sensor of 200 N capacity with accuracy of 0.1% full scale and an acoustic sensor 4381 V (Bruel & Kjear, Narum, Denmark) with a range from 1 kHz to 16 kHz. The acoustic sensor is placed inside the probe used for puncturing. The CAED punctures the fruit with a 11.1 mm diameter plunger which has a dome-shaped ending and a radius of curvature of 8.73 mm. This is pushed 8 mm into the apple with the speed of approximately 20 mm/min. Total full scale error of depth of penetration is approximately 0.5 mm. The signal from the acoustic sensor is recorded with a frequency of 44 kHz after hardware amplification and discrimination. The acoustic signal is converted on-line into counts which are the peaks higher than the discrimination level, found experimentally in a preliminary test, in such a way that background noise (when the motor drive of the device is switched off) is discriminated and noise from the motor drive when switched on gives ~600 counts/s, which is the bias of the method, whereas a typical number of counts for apple is of the order 104–106. In this experiment only the sum of all counts in the test, called total AE counts and firmness displayed on a LCD panel after the test, was taken for further analysis. The experiment was performed on apples after removing the skin.

Eleven apples of each cultivar were tested instrumentally and in sensory analysis.

## 3. Results

Fig. 1 presents examples of the height AFM images of the cell wall material (CWM) from investigated apple cultivars.

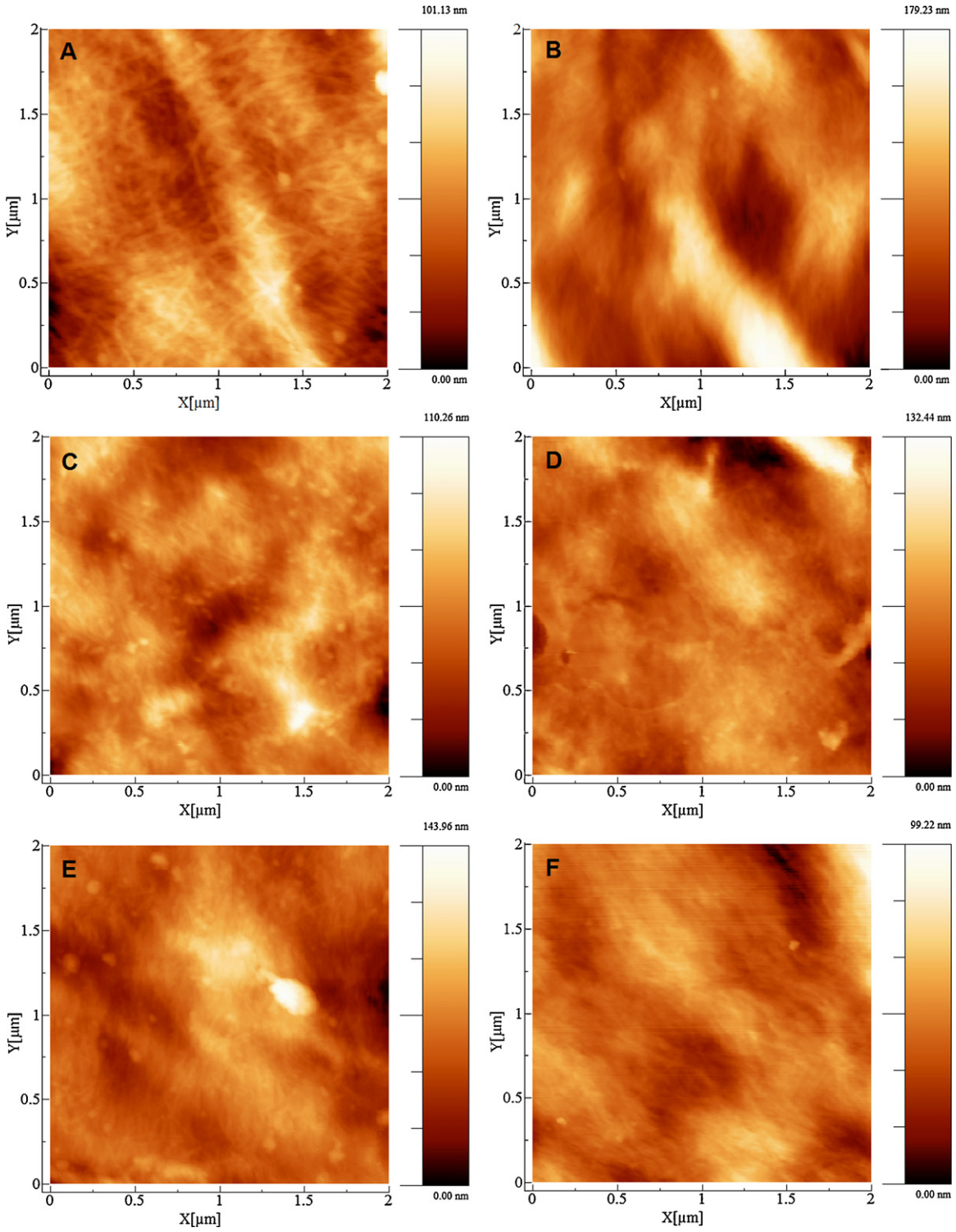


**Fig. 1.** The height images from atomic force microscope (AFM) in tapping mode revealing cell wall material (CWM) nanostructures for: (a) 'Cortland', (b) 'Honeycrisp', (c) 'Jonagold', (d) 'Ligol', (e) 'Mutsu' and (f) 'Rubin' apple cultivars.

In the images, cellulose microfibrils are barely visible as the brighter and elongated objects. The microfibrils are embedded in a pectin/hemicellulose matrix which caused image blurring and masking of the cellulose microfibrils. The height scale was taken mostly by the local unevenness of samples which was the most pronounced in the case of 'Honeycrisp' (Fig. 1b). Fig. 2 presents RMS roughness determined from the height images of CWM samples showing that the roughness of 'Honeycrisp' is significantly higher than other cultivars. The smallest roughness was obtained for 'Cortland', 'Jonagold' and 'Rubin', whereas 'Ligol' and 'Mutsu' revealed slightly higher roughness, but not as high as 'Honeycrisp'.

In general, the height images of CWM samples were not useful for estimation of the diameter of cellulose microfibrils due to the presence of the matrix polysaccharides. Therefore, in order to reveal the cellulose network, the pectin and hemicellulose matrix was removed. Fig. 3 presents examples of the height AFM images

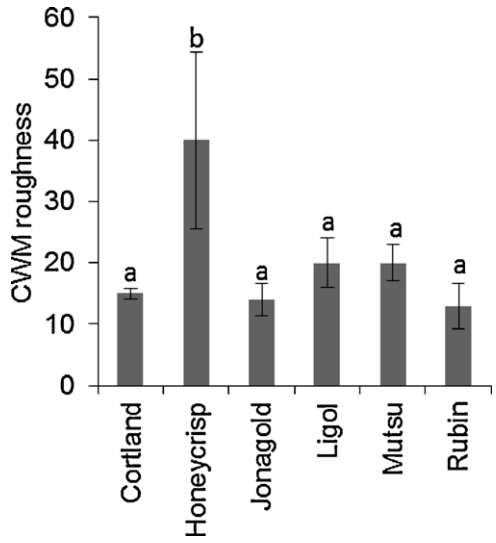


**Fig. 2.** Root-mean square roughness (nm) of cell wall material determined from the height AFM images of six apple cultivars. Error bars present standard deviations. The same letters above the bars mean no significant difference at $p = 0.05$.

of the cellulosic network of the investigated cultivars. The AFM images show a fine network of cellulose microfibrils which is more or less disordered. In the case of 'Cortland' (Fig. 3a) and 'Jonagold' (Fig. 3c) the microfibril orientation within the network seems to be very random, whereas the other cultivars show some preferences in the direction of fibril arrangement. From these height AFM images, the diameter of cellulose microfibrils was estimated (Fig. 4). It was performed in an objective way manually on 50 randomly chosen microfibrils for each cultivar. Fig. 4 shows that 'Honeycrisp' had the thickest cellulose microfibrils of about 38 nm. Then, 'Mutsu' had microfibrils which were significantly smaller in diameter (about 33 nm). The remaining cultivars had thinner microfibrils of about 26–28 nm. These values are comparable to former measurements of the diameter of cellulose microfibrils of natural and artificial cell walls (Cybulska, Konstankiewicz, et al., 2010).

Crystallinity was determined from the pure cellulose extracted, based on averaged diffractograms. Fig. 5a presents the calculated crystallinity of each apple cultivar showing that in this case 'Honeycrisp' cellulose microfibrils had the lowest crystallinity, whereas 'Jonagold' had the highest. Comparing this result with CWM roughness and the mean diameter of microfibrils, one can state that thicker microfibrils had a lower degree of crystallinity.

Pectin content determined from CWM is shown in Fig. 5b. The greatest pectins content was obtained for 'Ligol' then 'Rubin' and 'Honeycrisp'. Pectin content was found to be not correlated with the diameter of microfibrils, however, some regularity can be found with the degree of crystallinity (Fig. 5a). Cultivars with relatively low crystallinity, such as 'Honeycrisp' or 'Ligol', had higher pectin content, although it is not the rule in each case; an exception is 'Rubin' with both features being relatively high.

Fig. 6 presents sensory attributes evaluated in this experiment. Standard deviations were relatively large due to the subjective way of evaluation, despite training and discussion prior to testing. Post hoc analysis showed that only 'Cortland' and 'Rubin' differed significantly from the other cultivars. However, 'Honeycrisp' obtained the highest scores of crispness and juiciness, and the second highest score of hardness.

Sensory analysis is a very subjective method and a common problem of such evaluation is data scattering. Thus, different instrumental methods are explored to replace the sensory panel. Firmness is one of the simplest and also the most often used parameter for the quality evaluation of apples. It is also used for prediction of sensory texture. Fig. 7a presents the mean firmness of apples used in this experiment. The softest cultivars were 'Cortland' and 'Rubin', whereas 'Mutsu' was the firmest one, similarly so in the sensory analysis (Fig. 6b). The firmness of 'Honeycrisp' was higher than the firmness of 'Cortland', 'Jonagold' and 'Rubin', but not the highest among all the cultivars as one can expect from sensory analysis. In general, one can conclude that cultivars with higher sensory crispness, hardness and juiciness were also firmer. The particular properties of the 'Honeycrisp' cultivar are visible in Fig. 7b where mean total AE counts are depicted. 'Honeycrisp' revealed an unusually high number of AE counts recorded compared to other cultivars, whereas 'Cortland' and 'Rubin' had the smallest readings of this parameter. Comparing the two instrumental parameters, one can summarize that soft cultivars (low firmness) also had low acoustic emission, although 'Honeycrisp' presented different behaviour: it had high acoustic emission with average firmness, but in parallel this cultivar showed one of the highest sensory crispness and juiciness ratings.

To reveal relations among parameters measured in the experiment, principal component analysis on mean values was performed. Fig. 8 shows positions of samples and variables in the PCA graph along the first two components: PC1 and PC2. The two components explained in total 83% of the samples' variability. The scores plot (Fig. 8a) shows that 'Honeycrisp' had distinct properties from other cultivars. The group formed from 'Jonagold' and 'Mutsu' cultivars had negative values of PC2 and close to zero values of PC1. 'Cortland' and 'Rubin created the third group which was characterized by negative PC1 values and positive PC2 values. Comparing the scores plot (Fig. 8a) with the loadings plot (Fig. 8b), it is clear that in this data set, 'Honeycrisp' had positive influence on CWM roughness, cellulose diameter and all sensory and instrumental attributes. This cultivar also had a positive relation with pectin and a negative relation with cellulose crystallinity. 'Rubin' and 'Cortland' samples influenced negatively on texture attributes, CWM roughness and cellulose diameter. 'Jonagold' and 'Mutsu' cultivars were rather neutral for texture attributes within this group of cultivars, but were strongly positively influenced on crystallinity and negatively on pectin content locations in the PCA.

The loadings graph (Fig. 8b) provides a comprehensive view on the relation among variables measured in this experiment. Proximity of the parameters for CWM roughness, cellulose diameter and total AE counts shows high positive correlation among these variables. Similarly, sensory attributes (crispness, hardness and juiciness) are positioned close to firmness and relatively close to total AE counts and nanostructure parameters obtained from AFM (CWM roughness and cellulose diameter), showing their positive correlation. These variables did not correlate with the content of pectins, despite pectins being negatively correlated with cellulose crystallinity. Crystallinity correlated negatively with CWM roughness, cellulose diameter and total AE counts.

## 4. Discussion

At present, there is no commonly accepted biomechanical model of plant tissue, despite significant knowledge accumulated in this area. Texture of fruits and vegetables is determined by water and structural properties at various length scales. The mechanical properties of parenchyma tissue are controlled mainly by turgor, cell size, shape and packing, cell wall thickness and strength, and the extent of cell-to-cell adhesion (Toivonen & Brummell, 2008). Higher turgor causes increased tissue rigidity and brittleness (Zdunek & Bednarczyk, 2006). Tissue, if composed of smaller cells, has a larger content of cell walls, a lower relative amount of cytoplasm and vacuole, a greater area of cell-to-cell contact, a lower amount of intercellular spaces (Toivonen & Brummell, 2008)

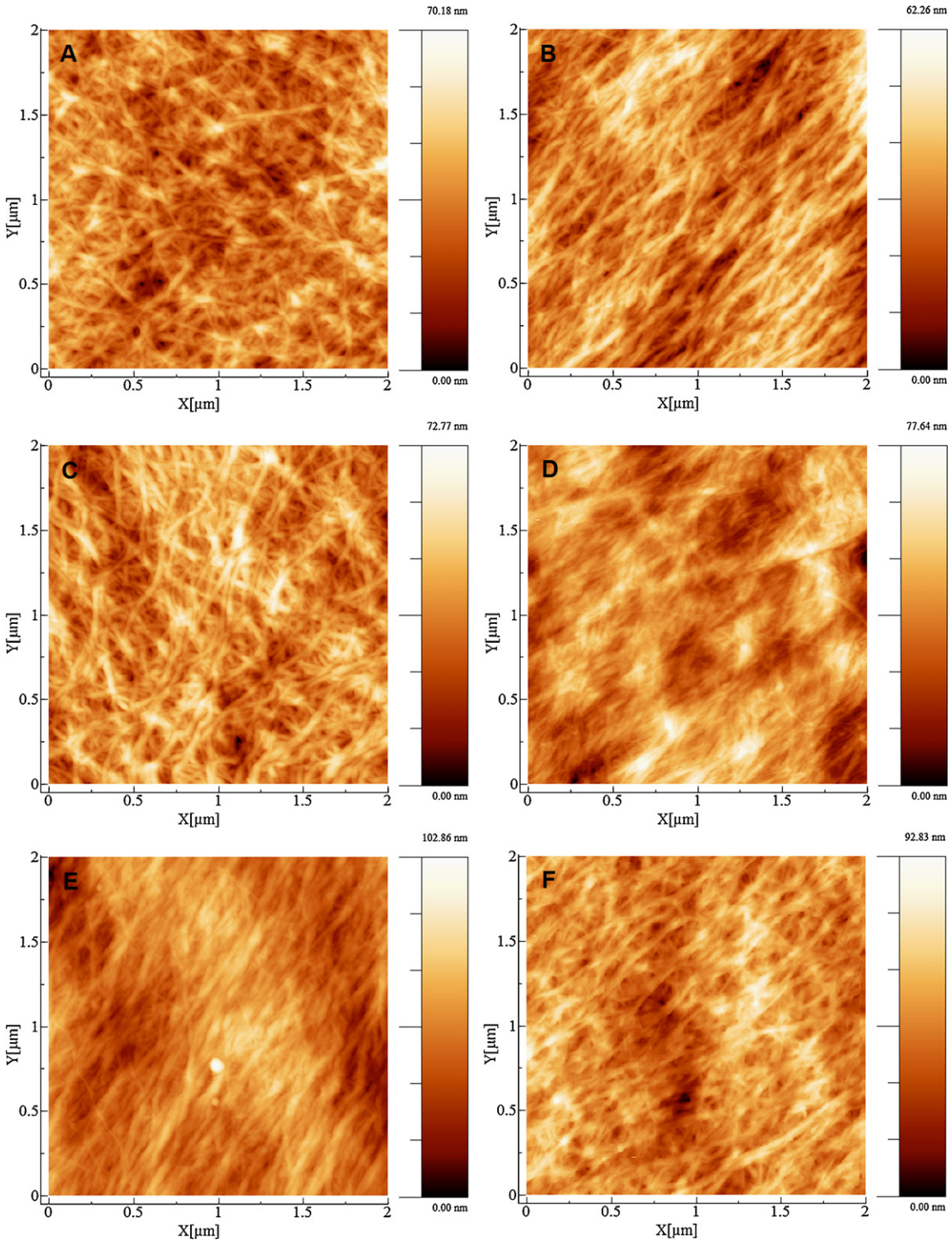


**Fig. 3.** The height images from AFM in tapping mode presenting cellulosic nanostructures of cell walls for: (a) 'Cortland', (b) 'Honeycrisp', (c) 'Jonagold', (d) 'Ligol', (e) 'Mutsu' and (f) 'Rubin' apple cultivars.

and such tissue reveals higher rigidity and strength for compression (Zdunek & Umeda, 2005). One of the roles of cell walls is to create, together with the middle lamella, a mechanical skeleton of tissue. The mechanical properties of cell walls depend on the polysaccharide composition (Cybulska, Vanstreels, et al., 2010), as well as their assembly and interlinkage (Jarvis, 2011).

Cell-to-cell adhesion plays a very significant role in the biomechanics of soft plant tissues (Jarvis, Briggs, & Knox, 2003) and, although is often interrelated to other structural properties of the tissue, it is also considered an important factor for the firmness and sensory texture of the fruit (Toivonen & Brummell, 2008). Crispy fruit tends to rupture through cells splitting open across

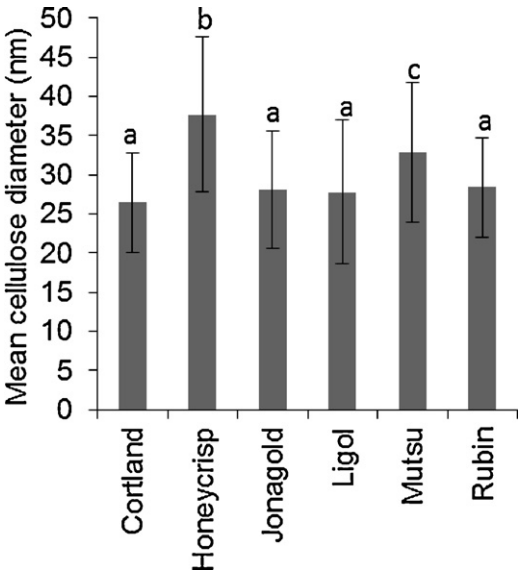


**Fig. 4.** Mean cellulose diameter of six apple cultivars. Error bars represent standard deviations from 50 manually chosen cellulose microfibrils from five AFM images. The same letters above the bars mean no significant difference at $p = 0.05$.

the primary cell walls (Harker, Stec, Hallett, & Bennett, 1997). However, cell separation may be a typical failure mode for soft fruit when ripe (De Belie, Hallett, Harker, & De Baerdemaeker, 2000). In the commonly accepted model of primary cell walls, hemicelluloses adhere to cellulose, cross-linking them to form a three-dimensional network which is imbedded in a matrix of pectic polysaccharides (Carpita & Gibeaut, 1993). Large changes occur in both pectins and matrix glycans during fruit ripening (Brummell, Dal Cin, Crisosto, & Labavitch, 2004). Among matrix glycans, glucomannans and xylans, which are weakly bound to cellulose, show little depolymerization compared to those tightly bound to cellulose (xyloglucan). During ripening, pectins become increasingly depolymerised and soluble (Redgwell, Curti, & Gehin-Delval, 2008). Depolymerization increases cell wall porosity, which initially may be low and may limit access of cell wall hydrolases to glycan substrates. During fruit ripening, pectins become increasingly de-esterified. Pectin de-esterification leads to loss of the integrity of cell walls, cell-to-cell adhesion, increase of intercellular spaces and a change of tissue structure.

The overview presented above shows that pectins are considered responsible for textural properties of the tissue, whereas the role of cellulose microfibrils in the mechanical characterization of fruit tissue is very often omitted. Cellulose is considered the most stable polymer; it is very strong for tension having the theoretical modulus of about 250 GPa (Vincent, 1999). Fruit ripening is related to structural changes of hemicelluloses and pectins. Thus, cellulose forms a kind of mechanical base of cell walls (Vincent, 1999). Therefore, the organization and dimensions of microfibrils are expected to play an important role in the mechanical properties of cell walls and also of tissue. This study showed that among cultivars of the same commodity there are significant differences in the cell wall composition. Among six cultivars studied, 'Honeycrisp' apples had a clearly distinct nanostructure of cell wall from others. It had the thickest cellulose microfibrils and the lowest crystallinity. Oppositely, 'Cortland' and 'Rubin' had the thinnest microfibrils and high (not the highest) crystallinity. This is important when compared with sensory and instrumental texture. 'Honeycrisp' was scored as a very crisp, juicy and hard fruit, whereas 'Cortland' and 'Rubin' were scored as soft and "silent". This suggests that crisper, harder and juicier fruits have thicker microfibrils and lower crystallinity (Fig. 8). Such apples also emit abundant sound during puncturing (high total AE counts), however, it is not always clearly related to higher firmness. The mechanism of crispness and juiciness is related with cell wall rupturing (Waldron, Smith, Parr, Ng, & Parker, 1997). When a turgid cell is compressed, the cell wall breaks, generating sound waves due to the somehow elastic properties of walls. The amplitude of the elastic waves is proportional to the stress in the moment of rupture (Malecki & Opilski, 1994). Presumably thicker microfibrils cause the failure stress of the cell wall to be higher and increase the crispness sense and total AE count – as was observed in this experiment. The hypothesis that the diameter of microfibrils influences the texture is supported by the relation to hardness. Similarly, thicker cellulose microfibrils correspond to harder tissue due to the increase of cell wall tensile strength.

Cellulose crystallinity, obtained by X-ray diffraction, was slightly lower compared to the value of 25% for 'Ligol' apples obtained previously by the FT-IR method (Szymanska-Chargot, Cybulska, & Zdunek, 2011) but this study showed that the level depends on the cultivar. In general, the degree of crystallinity obtained here are very low compared to bacterial cellulose (40–50%) and microcrystalline cellulose (>50%) (Szymanska-Chargot et al., 2011). Thicker microfibrils were less crystalline, thus, the crystallinity level tends to correlate negatively with the texture. Crystal parts of microfibrils are very stable and strong, thus, one can

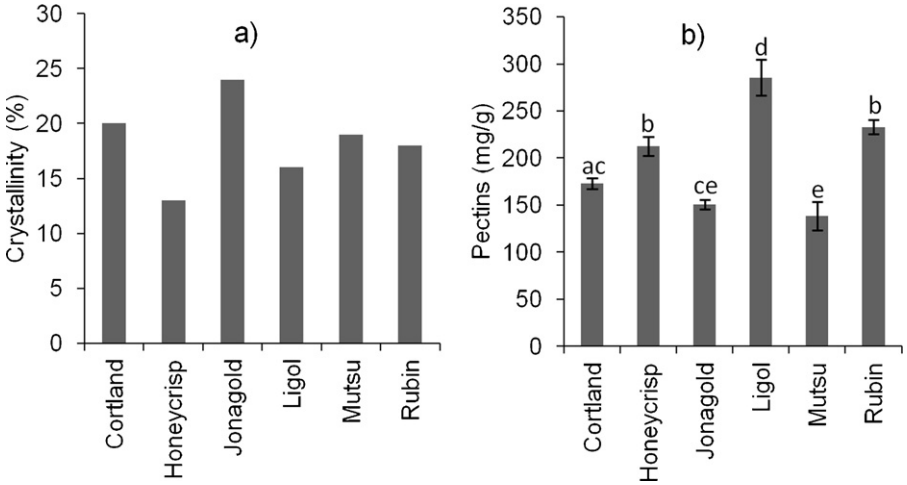


**Fig. 5.** (a) Degree of crystallinity of cellulose determined by X-ray diffraction for cell wall material from six different apple cultivars. (b) Pectin content of six apple cultivars. Error bars represent standard deviations from three replicates. The same letters above the bars mean no significant difference at $p = 0.05$.

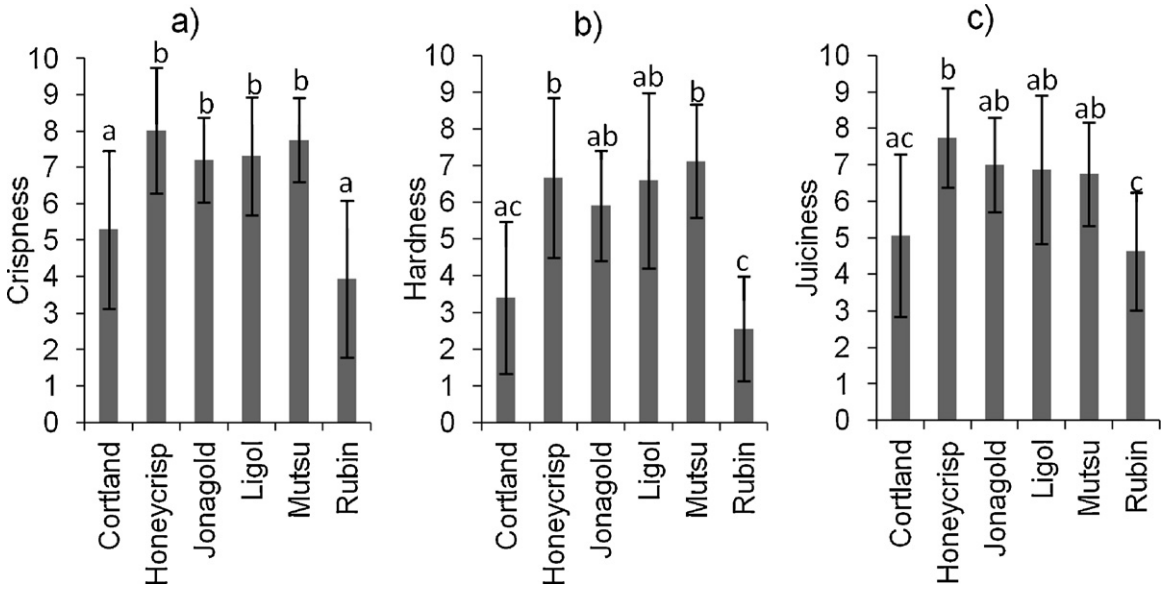


**Fig. 6.** Mean sensory texture attributes of six apple cultivars: (a) crispness, (b) hardness and (c) juiciness. Error bars depict standard deviations from 10 apples (each panellist tested one apple). The same letters above the bars mean no significant difference at $p = 0.05$.

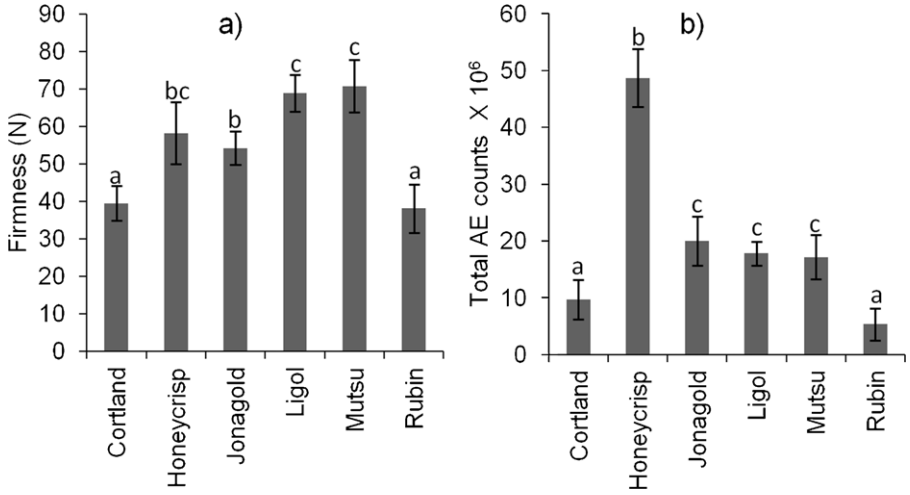


**Fig. 7.** Mean mechanical parameters of six apple cultivars: (a) firmness and (b) total AE events. Bars show standard deviations from 10 apples (one measurement per apple). The same letters above the bars mean no significant difference at $p = 0.05$.

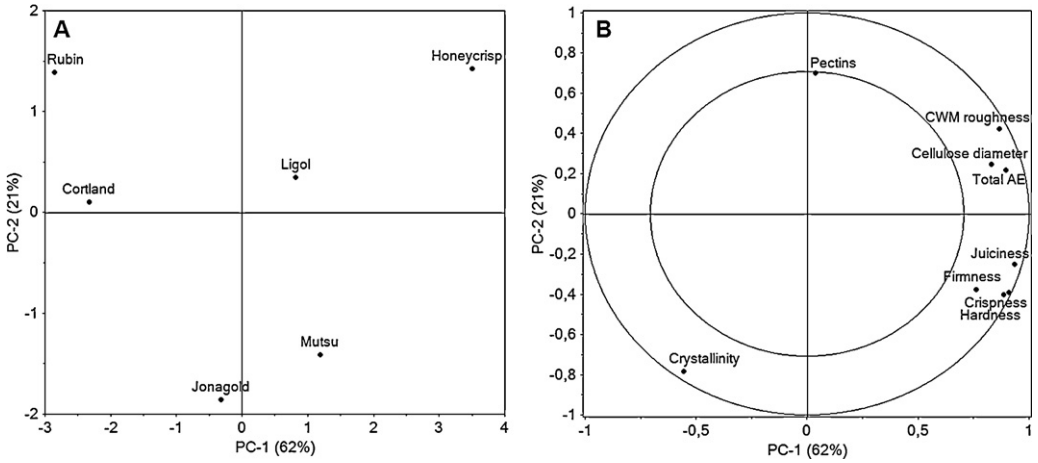


**Fig. 8.** Joint principal component analysis (along PC1 and PC2) of sensory evaluation (crispness, hardness and juiciness), mechanical properties (firmness and total AE counts), and cell wall nanostructure characteristics (CWM roughness, cellulose diameter of microfibrils, crystallinity and pectin content) for six apple cultivars, (a) scores plot, and (b) loadings plot.

expect that the mechanical strength of tissue should correlate positively with the crystallinity level. The negative relation, obtained in this study, suggests that this is not straightforward. Presumably, lower crystallinity of thicker microfibrils was caused by the higher contribution of the amorphous part which surrounded the crystalline core (Vincent, 1999). It is not a simple case of proposing a simple interpretation of the apparent relation of microfibril diameter and crystallinity with juiciness. One can expect that higher cell wall strength would mean fewer cells split open, thus, juiciness should decrease. On the other hand, juiciness usually correlates positively with crispness and hardness, so the results here are in line with those previously reported (Zdunek et al., 2010).

In this work, an attempt was made to compare the nanostructure of cell walls with macro-textural properties. Important micro-properties of cell walls, like turgor, cell and intercellular size, tissue heterogeneity and cell-to-cell integrity were omitted in the analysis. This must be included in future studies to perform a more comprehensive analysis of structural factors determining the texture of fruits. Presumably, an important part of data variability would be explained by micro-structural and biochemical differences among cultivars, although this experiment showed that significant differences in nanostructure of cell walls must be considered in a model of the mechanical properties of fruits and in an explanation of their texture. The experiment has shown an evidence of relationship between macroscopic sensory and instrumental texture and the nanostructure of apple tissue but deeper study on properties of individual fruit at various scales is still needed. Sensory analysis is typical macro-scale property where a batch of fruits is tested by group of panellists to obtain consistent data. The relation of sensory data with properties at nanoscale may be affected and hidden by many aforementioned properties at cellular and tissue level. Therefore, consistent explanation of sensory texture requires further study of mechanical properties and structure of fruits at multiple scales.

## 5. Conclusions

The AFM study of the nanostructure of cell walls shows that apple cultivars differ in terms of cellulose diameter and crystallinity, and pectin content. Cultivars with thicker cellulose microfibrils also revealed a crisper, harder and juicier texture, and greater acoustic emission. The results suggest that microfibril thickness affects the mechanical strength of cell walls which has consequences for sensory and instrumental texture. This suggestion shows the necessity to include the nanostructural properties of cell walls in a biomechanical multiscale model of plant tissue. For fruits particularly, it would help to explain individual textural properties and would complete the rich data collected on the dynamic changes that occur during pre- and post-harvest ripening.

## Acknowledgements

This work was partly funded by The Norwegian Research Council (Project No. 195777) and The Polish National Budget for Science 2010-2011 (Project No. IP2010 005770) and the authors would like to acknowledge their support.

## References

Aguilera, J. M. (2005). Why food microstructure? *Journal of Food Engineering*, *67*, 3–11.

Blumenkrantz, N., & Asboe-Hansen, G. (1973). New method for quantitative determination of uronic acid. *Analytical Biochemistry*, *54*, 484–489.

Brummell, D. A., & Harpster, M. H. (2001). Cell wall metabolism in fruit softening and quality and its manipulation in transgenic plants. *Plant Molecular Biology*, *47*, 311–340.

Brummell, D. A., Dal Cin, V., Crisosto, C. H., & Labavitch, J. M. (2004). Cell wall metabolism during maturation ripening and senescence of peach fruit. *Journal of Experimental Botany*, *55*, 2029–2039, 405.

Carpita, N. C., & Gibeaut, D. M. (1993). Structural models of primary cell walls in flowering plants: Consistency of molecular structure with the physical properties of the walls during growth. *Plant Journal*, *3*, 1–30.

Chen, F., Zhang, L., An, H., Yang, H., Sun, X., Liu, H., et al. (2009). The nanostructure of hemicellulose of crisp and soft Chinese cherry (*Prunus pseudocerasus* L.) cultivars at different stages of ripeness. *LWT: Food Science and Technology*, *42*, 125–130.

Chen, F., Liu, H., Yang, H., Lai, S., Cheng, X., Xin, Y., et al. (2011). Quality attributes and cell wall properties of strawberries (*Fragaria annanassa* Duch.) under calcium chloride treatment. *Food Chemistry*, *126*, 450–459.

Cybulska, J., Vanstreels, E., Ho, Q. T., Courtin, C. M., Van Craeyveld, V., Nicolaï, B., et al. (2010). Mechanical characteristics of artificial cell walls. *Journal of Food Engineering*, *96*, 287–294.

Cybulska, J., Konstankiewicz, K., Zdunek, A., & Skrzypiec, K. (2010). Nanostructure of natural apple cell wall and model cell wall materials. *International Agrophysics*, *24*, 107–114.

Cybulska, J., Zdunek, A., & Konstankiewicz, K. (2011). Calcium effect on mechanical properties of model cell walls and apple tissue. *Journal of Food Engineering*, *102*, 217–223.

Davies, L. M., & Harris, P. J. (2003). Atomic force microscopy of microfibrils in primary cell walls. *Planta*, *217*, 283–289.

De Belie, N., Hallett, I. C., Harker, F. R., & De Baerdemaeker, J. (2000). Influence of ripening and turgor on the tensile properties of pears: A microscopic study of cellular and tissue changes. *Journal of the American Society for Horticultural Science*, *125*, 350–356.

Ding, S.-Y., & Himmel, M. E. (2006). The maize primary cell wall microfibril: A new model derived from direct visualization. *Journal of Agricultural and Food Chemistry*, *54*, 597–606.

Fishman, M. L., Cooke, P. H., & Coffin, D. R. (2006). Nanostructure of native pectin sugar acid gels visualized by atomic force microscopy. *Biomacromolecules*, *5*, 334–341.

Harker, F. R., Stec, M. G. H., Hallett, I. C., & Bennett, C. L. (1997). Texture of parenchymatous plant tissue: A comparison between tensile and other instrumental and sensory measurements of tissue strength and juiciness. *Postharvest Biology and Technology*, *11*, 63–72.

Horcas, I., Fernandez, R., Gomez-Rodriguez, J. M., Colchero, J., Gomez-Herrero, J., & Baro, A. M. (2007). WSXM: A software for scanning probe microscopy and a tool for nanotechnology. *Review of Scientific Instruments*, *78*, 013705.

Jarvis, M. C. (2011). Plant cell walls: Supramolecular assemblies. *Food Hydrocolloids*, *25*, 257–262.

Jarvis, M. C., Briggs, S. P. H., & Knox, J. P. (2003). Intercellular adhesion and cell separation in plants. *Plant, Cell and Environment*, *26*, 977–989.

Kirby, A. R., Gunning, A. P., Waldron, K. W., Morris, V. J., & Ng, A. (1996). Visualization of plant cell walls by atomic force microscopy. *Biophysical Journal*, *70*, 1138–1143.

Kirby, A. R., MacDougall, A. J., & Morris, V. J. (2008). Atomic force microscopy of tomato and sugar beet pectin molecules. *Carbohydrate Polymers*, *71*, 640–647.

Konopacka, D., & Płocharski, W. J. (2004). Effect of storage conditions on the relationship between apple firmness and texture acceptability. *Postharvest Biology and Technology*, *32*(2), 205–211.

Lawless, H. T., & Heymann, H. (2010). *Sensory evaluation of food. principles and practices*. New York: Springer Science + Business Media., pp. 240–247.

Liu, H., Chen, F., Yang, H., Yao, Y., Gong, X., Xin, Y., et al. (2009). Effect of calcium treatment on nanostructure of chelate-soluble pectin and physicochemical and textural properties of apricot fruits. *Food Research International*, *42*, 1131–1140.

Liu, H., Fu, S., Zhu, J. Y., Li, H., & Zhan, H. (2009). Visualization of enzymatic hydrolysis of cellulose using AFM phase imaging. *Enzyme and Microbial Technology*, *45*, 274–281.

Malecki, I., & Opilski, A. (1994). Characteristics and classification of acoustic emission signals. In I. Malecki, & J. Ranachowski (Eds.), *Acoustic emission: Sources, methods and applications* (pp. 18–33). Warszawa: Wyd. Biuro PASCAL (in Polish).

Marga, F., Grandbois, M., Cosgrove, D. J., & Baskin, T. I. (2005). Cell wall extension results in the coordinate separation of parallel microfibrils: Evidence from scanning electron microscopy and atomic force microscopy. *Plant Journal*, *43*, 181–190.

Morris, V. J., Guning, A. P., Kirby, A. R., Round, A., Waldron, K., & Ng, A. (1997). Atomic force microscopy of plant cell walls, plant cell wall polysaccharides and gels. *International Journal of Biological Macromolecules*, *21*, 61–66.

Redgwell, R. J., Curti, D., & Gehin-Delval, C. (2008). Role of pectic polysaccharides in structural integrity of apple cell wall material. *European Food Research and Technology*, *227*, 1025–1033.

Redgwell, R. J., Melton, L. D., & Brasch, D. J. (1988). Cell wall polysaccharides of kiwifruit (*Actinidia deliciosa*): Chemical features in different tissue zones of the fruit at harvest. *Carbohydrate Research*, *182*, 241–258.

Renard, C. M. G. C. (2005). Variability in cell wall preparations, quantification and comparison of common methods. *Carbohydrate Polymers*, *60*, 512–522.

Round, A. N., Rigby, N. M., MacDougall, A. J., & Morris, V. J. (2010). A new view of pectin structure revealed by acid hydrolysis and atomic force microscopy. *Carbohydrate Research*, *345*, 487–497.

Szymanska-Chargot, M., Cybulska, J., & Zdunek, A. (2011). Sensing the structural differences in cellulose from apple and bacterial cell wall materials by Raman and FT-IR spectroscopy. *Sensors*, *11*, 5543–5560.

Thimm, J. C., Burritt, D. J., Ducker, W. A., & Melton, L. D. (2000). Celery (*Opium graveolens* L.) parenchyma cell walls by atomic force microscopy: Effect of dehydration on cellulose microfibrils. *Planta*, *212*, 25–32.

Toivonen, P. M. A., & Brummell, D. A. (2008). Biochemical bases of appearance and texture changes in fresh-cut fruit and vegetables. *Postharvest Biology and Technology*, *48*, 1–14.

Vincent, J. F. V. (1999). From cellulose to cell. *The Journal of Experimental Biology*, *202*, 3263–3268.

Waldron, K. W., Smith, A. C., Parr, A. J., Ng, A., & Parker, M. L. (1997). New approaches to understanding and controlling cell separation in relation to fruit and vegetable texture. *Trends in Food Science and Technology*, *8*, 213–221.

Wunderlich, B. (1973). *Macromolecular physic*. New York: Academic Press.

Yang, H., An, H., Feng, G., Li, Y., & Lai, S. (2005). Atomic force microscopy of the water-soluble pectin of peaches during storage. *European Food Research and Technology*, *220*, 587–591.

Zdunek, A., & Bednarczyk, J. (2006). Effect of mannitol treatment on ultrasound emission during texture profile analysis of potato and apple tissue. *Journal of Texture Studies*, *37*, 339–359.

Zdunek, A., & Umeda, M. (2005). Influence of cell size and cell wall volume fraction on failure properties of potato and carrot tissue. *Journal of Texture Studies*, *36*, 25–43.

Zdunek, A., Cybulska, J., Konopacka, D., & Rutkowski, K. (2010). New contact acoustic emission detector for texture evaluation of apples. *Journal of Food Engineering*, *99*, 83–91.

Zdunek, A., Cybulska, J., Konopacka, D., & Rutkowski, K. (2011a). Inter-laboratory analysis of firmness and sensory texture of stored apples. *International Agrophysics*, *25*(1), 67–75.

Zdunek, A., Cybulska, J., Konopacka, D., & Rutkowski, K. (2011b). Evaluation of apple texture with contact acoustic emission detector: A study on performance of calibration models. *Journal of Food Engineering*, *106*, 80–87.

Zhang, L., Chen, F., Yang, H., Ye, X., Sun, X., Liu, D., et al. (2012). Effects of temperature and cultivar on nanostructural changes of water-soluble pectin and chelate-soluble pectin in peaches. *Carbohydrate Polymers*, *87*, 816–821.

Zhang, L., Chen, F., Yang, H., Sun, X., Liu, H., Gong, X., et al. (2010). Changes in firmness, pectin content and nanostructure of two crisp peach cultivars after storage. *LWT: Food Science and Technology*, *43*, 26–32.

Żykwińska, A., Thibault, J.-F., & Ralet, M.-C. (2008). Competitive binding of pectin and xyloglucan with primary cell wall cellulose. *Carbohydrate Polymers*, *74*, 957–961.